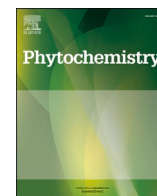




Contents lists available at ScienceDirect

## Phytochemistry

journal homepage: [www.elsevier.com/locate/phytochem](http://www.elsevier.com/locate/phytochem)Squamins C–F, four cyclopeptides from the seeds of *Annona globiflora*

Javier Sosa-Rueda<sup>a</sup>, Vaniamin Domínguez-Meléndez<sup>b</sup>, Araceli Ortiz-Celiseo<sup>a,c</sup>,  
 Fernando C. López-Fentanes<sup>a</sup>, Cristina Cuadrado<sup>d</sup>, José J. Fernández<sup>e,\*</sup>,  
 Antonio Hernández Daranas<sup>d,\*\*\*</sup>, Francisco Cen-Pacheco<sup>a,e,\*</sup>

<sup>a</sup> Facultad de Bioanálisis, Veracruz University, Iturbide s/n, 91700, Veracruz, Ver., Mexico<sup>b</sup> Centro de Estudios y Servicios en Salud, Veracruz University, Iturbide s/n, 91700, Veracruz, Ver., Mexico<sup>c</sup> Instituto Tecnológico de Orizaba, Tecnológico Nacional de México Oriente 9, Emiliano Zapata, 94320, Orizaba, Ver., Mexico<sup>d</sup> Instituto de Productos Naturales y Agrobiología del CSIC (IPNA-CSIC), La Laguna, 38206, Tenerife, Spain<sup>e</sup> Instituto Universitario de Bio-Organica Antonio González (IUBO-AG), Departamento de Química Orgánica, University of La Laguna, Av. Astrofísico Francisco Sánchez 2, 38206, Tenerife, Spain

## ARTICLE INFO

## Keywords:

*Annona globiflora* Schltld.  
 Annonaceae  
 Cyclopeptides  
 Cytotoxic activity

## ABSTRACT

Four cyclic octapeptides, squamins C–F, were isolated from the seeds of *Annona globiflora* Schltld. These compounds share part of their amino acid sequence, -Pro-Met(O)-Tyr-Gly-Thr-, with previously reported squamins A and B. Their structures were determined using NMR spectroscopic techniques together with quantum mechanical calculations (QM-NMR), ESI-HRMS data and a modified version of Marfey's chromatographic method. All compounds showed cytotoxic activity against DU-145 (human prostate cancer) and HeLa (human cervical carcinoma) cell lines. Clearly, *A. globiflora* is an important source of bioactive molecules, which could promote the sustainable exploitation of this undervalued specie.

## 1. Introduction

In Mexico, there are about 20 species of *Annona* genus, mainly located in southeastern tropical regions. *Annona muricata* L. (Annonaceae) is one the most cultivated species of the *Annona* genus, because it produces exotic edible fruits (Anaya-Esparza et al., 2020). However, the economic importance of this genus is diverse and not restricted to their fruits, as it also includes species with aromatic, medicinal and insecticidal properties (Hernández Vidal et al., 2014). Despite this, most of them are known as wild *Annona* species (Anaya-Esparza et al., 2020) and remain underutilized. Within this group of wild native *Annona* species, we focused the current study on *Annona globiflora* Schltld. (Annonaceae). This Mexican endemic species is named “chirimoyito” by local people, and grows in the central area of the state of Veracruz (Escobedo-López et al., 2018). To our knowledge, previous studies of its phytochemistry or biological activity have not been reported.

The *Annona* genus is well known for producing interesting compounds, including alkaloids, isoquinolines, peptides, acetogenins, lectins, volatile oils, etc. (Leite et al., 2020). Cyclic peptides isolated from

the genus *Annona* constitute an important class of natural molecules with a great diversity of ring sizes (Dahiya and Dahiya, 2021). Some of them show useful pharmacologic properties such as potent cytotoxic, vasorelaxant or anti-inflammatory activities (Cen-Pacheco et al., 2019b). Consequently, they have been described as interesting leads in the drug discovery process (Anaya-Esparza et al., 2020; Dahiya and Dahiya, 2021). Therefore, knowledge of the functional potential of wild native *Annona* species, and evidence on the possible health benefits derived from them, may promote the expansion of their cultivation and commercial importance.

Here, we report a phytochemical study of the seeds of *A. globiflora* collected in spring 2018 in Veracruz state (México), in which four previously unreported cyclopeptides named squamins C–F (1–4) were isolated. Their structures were determined using NMR spectroscopic techniques together with quantum mechanical calculations (QM-NMR) (Daranas and Sarotti, 2021), ESI-HRMS data and a modified version of Marfey's method using LC-UV (Unno et al., 2020; Bhushan and Brückner, 2004). Squamins C/D and E/F were found to be pairs of epimeric methionine sulfoxides, which may be oxidation products of undetected

\* Corresponding author.

\*\* Corresponding author.

\*\*\* Corresponding author.

E-mail address: [fcen@uv.mx](mailto:fcen@uv.mx) (F. Cen-Pacheco).<https://doi.org/10.1016/j.phytochem.2021.112839>

Received 10 December 2020; Received in revised form 22 May 2021; Accepted 10 June 2021

0031-9422/© 2021 The Authors. Published by Elsevier Ltd. This is an open access article under the CC BY license (<http://creativecommons.org/licenses/by/4.0/>).

cyclopeptides containing *L*-Met. Importantly, unlike other compounds containing a methionine sulfoxide group, squamins can be separated by chromatographic techniques (Capon, 2020). The cytotoxicity bioassays undertaken indicated that these compounds possess moderate activity against the DU-145 (human prostate cancer) and HeLa (human cervical carcinoma) cell lines.

## 2. Results and discussion

### 2.1. Extraction and isolation

Seeds of *Annona globiflora* (500 g) were dried under shade and triturated using a steel blender. Next, the resulting powder was extracted using MeOH (4 × (3 L × 3 h)) at room temperature and the solvent evaporated *in vacuo* to yield a brownish viscous extract (12.5 g). This extract was first fractionated by liquid-liquid extraction, using the modified Kupchan method (Kupchan et al., 1973; Cen-Pacheco et al., 2019a,b). The AcOEt fraction (416 mg) was chromatographed using medium pressure liquid chromatography Lobar LiChroprep-RP18 with MeOH/H<sub>2</sub>O 7:3, then finally purified in a  $\mu$ -Bondapack C-18 HPLC column using MeOH:H<sub>2</sub>O as mobile phase. This procedure yielded 2.9 mg of squamin C (1), 2.5 mg of squamin D (2), 1.9 mg of squamin E (3) and 1.5 mg of squamin F (4).

### 2.2. Structural elucidation

Squamin C (1) was isolated as an optically active amorphous white solid [ $\alpha$ ]<sub>D</sub><sup>25</sup> -52 (*c* = 0.29, MeOH). ESI-HRMS mass spectra showed a molecular ion peak [M+Na]<sup>+</sup> at *m/z* 843.3691, providing the molecular formula C<sub>37</sub>H<sub>56</sub>N<sub>8</sub>O<sub>11</sub>S. The NMR spectroscopic data were obtained using CD<sub>3</sub>OD and CD<sub>3</sub>OH as solvents. The observed <sup>1</sup>H and <sup>13</sup>C NMR data for 1 allowed us to establish the presence of six CH<sub>3</sub>, eight CH<sub>2</sub>, thirteen CH and ten non-protonated carbons. Importantly, eight signals characteristic of carbonyl groups were observed in the <sup>13</sup>C NMR spectrum, suggesting that 1 should be an octapeptide (Table 1). Indeed, <sup>1</sup>H-<sup>1</sup>H COSY and TOCSY spectra of 1 revealed the presence of nine <sup>1</sup>H-<sup>1</sup>H spin systems, belonging to eight amino acid units. Thus, two alanine residues showed the typical AX<sub>3</sub> system between H<sub>3</sub>-β (δ<sub>H</sub> 1.42, *d*, *J* = 7.3 Hz) and H-α (δ<sub>H</sub> 3.99, *q*, *J* = 7.3 Hz) and between H<sub>3</sub>-β (δ<sub>H</sub> 1.44, *d*, *J* = 7.4 Hz) and H-α (δ<sub>H</sub> 4.22, *q*, *J* = 7.4 Hz). The *sec*-butyl group of the isoleucine residue was identified, beginning with proton H-α (δ<sub>H</sub> 4.37, *d*, *J* = 10.4 Hz). This was correlated with the methine proton H-β (δ<sub>H</sub> 2.09), then in turn with the methyl group H<sub>3</sub>-ε (δ<sub>H</sub> 0.77, *d*, *J* = 6.5 Hz) and the diastereotopic methylene H<sub>2</sub>-γ (δ<sub>H</sub> 1.07/1.49). The latter was further correlated with H<sub>3</sub>-δ (δ<sub>H</sub> 0.94, *t*, *J* = 7.4 Hz). The proline residue started with H-α (δ<sub>H</sub> 4.74, *dd*, *J* = 7.9, 9.7 Hz). This was linked to H<sub>2</sub>-β (δ<sub>H</sub> 1.91/2.34), this in turn to H<sub>2</sub>-γ (δ<sub>H</sub> 2.08) and the latter to H<sub>2</sub>-δ (δ<sub>H</sub> 3.57/3.75). The <sup>1</sup>H NMR signal assignment of the non-essential amino acid, methionine oxide, commenced with H-α (δ<sub>H</sub> 4.20, *t*, *J* = 7.1 Hz), which was connected to H<sub>2</sub>-β (δ<sub>H</sub> 2.06/2.21) and these sequentially to H<sub>2</sub>-γ (δ<sub>H</sub> 2.60/2.67). For the tyrosine residue, two-spin systems were determined: the first linked H-α (δ<sub>H</sub> 5.02, *dd*, *J* = 3.0, 12.4 Hz) with H<sub>2</sub>-β (δ<sub>H</sub> 2.85/3.62, *dd/dd*, *J* = 12.4, 15.8 Hz/*J* = 3.0, 15.7 Hz), while the second joined protons H-δ/H-θ (δ<sub>H</sub> 7.04, *d*, *J* = 8.5 Hz) with H-ε/H-η (δ<sub>H</sub> 6.71, *d*, *J* = 8.5 Hz). Observation of a <sup>1</sup>H-<sup>1</sup>H spin coupling between two geminal protons H<sub>2</sub>-α (δ<sub>H</sub> 3.74/4.27, *d*, *J* = 17.1 Hz) indicated the presence of a glycine residue. Finally, the threonine residue began at H<sub>3</sub>-γ (δ<sub>H</sub> 1.23, *d*, *J* = 6.1 Hz), which was joined with methine H-β (δ<sub>H</sub> 4.52, *dq*, *J* = 3.1, 6.1 Hz), and this sequentially connected with H-α (δ<sub>H</sub> 4.89, *d*, *J* = 3.1 Hz). The peptide sequence was unambiguously established by long-range <sup>1</sup>H-<sup>13</sup>C connectivity, extrapolated from the HMBC experiment. This further secured the presence of eight amino acid residues in 1. Thus, key HMBC correlations between the carbonyl group of residue *i* and the amide and/or α protons of residue *i*+1 (Ala<sup>1</sup>H-α and Thr(CO), Ala<sup>2</sup>H-α and Ala<sup>1</sup>(CO), IleH-α and Ala<sup>2</sup>(CO), ProH-α and Ile(CO), Met(O)H-α and Pro(CO),

**Table 1**

NMR data (CD<sub>3</sub>OH) for squamins C (1) and D (2).

| Amino acid       | Position         | Squamin C (1)        |  | Squamin D (2)        |  |
|------------------|------------------|----------------------|--|----------------------|--|
|                  |                  | δ <sub>c</sub>       | δ <sub>H</sub> , mult. ( <i>J</i> in Hz) | δ <sub>c</sub>       | δ <sub>H</sub> , mult. ( <i>J</i> in Hz) |
| Ala <sup>1</sup> | CO               | 176.6                |  | 176.6                |  |
|                  | αCH              | 53.1                 | 3.99, <i>q</i> (7.3)                     | 53.1                 | 3.95, <i>q</i> (7.3)                     |
|                  | βCH <sub>3</sub> | 16.4                 | 1.42, <i>d</i> (7.3)                     | 16.4                 | 1.38, <i>d</i> (7.3)                     |
|                  | NH               |                      | 7.50                                     |                      |  |
| Ala <sup>2</sup> | CO               | 175.8                |  | 175.8                |  |
|                  | αCH              | 52.4                 | 4.22, <i>q</i> (7.4)                     | 52.4                 | 4.19, <i>q</i> (7.4)                     |
|                  | βCH <sub>3</sub> | 17.7                 | 1.44, <i>d</i> (7.4)                     | 17.7                 | 1.41, <i>d</i> (7.4)                     |
|                  | NH               |                      | 7.50, <i>bs</i>                          |                      | 7.51, <i>bs</i>                          |
| Ile              | CO               | 172.6                |  | 172.6                |  |
|                  | αCH              | 56.8                 | 4.37 <i>d</i> (10.4)                     | 56.8                 | 4.35 <i>d</i> (10.4)                     |
|                  | βCH              | 37.2                 | 2.09 <i>m</i>                            | 37.2                 | 2.07 <i>m</i>                            |
|                  | γCH <sub>2</sub> | 25.1                 | 1.07 <i>m</i>                            | 25.1                 | 1.05 <i>m</i>                            |
|                  |                  |                      | 1.49 <i>m</i>                            |                      | 1.47 <i>m</i>                            |
|                  | δCH <sub>3</sub> | 11.7                 | 0.94 <i>t</i> (7.4)                      | 11.6                 | 0.92 <i>t</i> (7.4)                      |
|                  | εCH <sub>3</sub> | 18.4                 | 0.77 <i>d</i> (6.5)                      | 18.0                 | 0.75 <i>d</i> (6.5)                      |
|                  | NH               |                      | 7.31 <i>d</i> (9.4)                      |                      | 7.32 <i>d</i> (9.4)                      |
| Pro              | CO               | 178.0                |  | 178.0                |  |
|                  | αCH              | 64.8                 | 4.74 <i>dd</i> (7.9, 9.7)                | 64.7                 | 4.71 <i>dd</i> (4.0, 7.7)                |
|                  | βCH <sub>2</sub> | 30.5                 | 1.91 <i>m</i>                            | 30.5                 | 1.90 <i>m</i>                            |
|                  |                  |                      | 2.34 <i>ddt</i> (5.0, 7.9, 12.5)         |                      | 2.32 <i>m</i>                            |
| Met(O)           | CO               | 173.7                |  | 173.6                |  |
|                  | αCH              | 56.3                 | 4.20 <i>t</i> (7.1)                      | 56.6                 | 4.13 <i>dd</i> (6.1, 7.3)                |
|                  | βCH <sub>2</sub> | 24.3                 | 2.06 <i>m</i>                            | 25.3                 | 2.04 <i>m</i>                            |
|                  |                  |                      | 2.21 <i>m</i>                            |                      | 2.19 <i>m</i>                            |
| Tyr              | γCH <sub>2</sub> | 49.6                 | 2.60 <i>m</i>                            | 50.0                 | 2.60 <i>m</i>                            |
|                  |                  |                      | 2.67 <i>m</i>                            |                      | 2.64 <i>m</i>                            |
|                  | δCH <sub>3</sub> | 37.5                 | 2.47 <i>s</i>                            | 37.9                 | 2.56 <i>s</i>                            |
|                  | CO               | 174.2                |  | 174.2                |  |
|                  | αCH              | 53.7                 | 5.02, <i>dd</i> (3.0, 12.4)              | 53.8                 | 4.99, <i>ddd</i> (3.0, 10.0, 12.6)       |
|                  | βCH <sub>2</sub> | 36.8                 | 2.85, <i>dd</i> (12.4, 15.8)             | 36.9                 | 2.82, <i>dd</i> (12.6, 15.8)             |
|                  |                  |                      | 3.62, <i>dd</i> (3.0, 15.7)              |                      | 3.61, <i>dd</i> (3.0, 15.8)              |
|                  | γC               | 129.1                |  | 129.6                |  |
| δCH/θCH          | 130.1            | 7.04, <i>d</i> (8.5) | 130.2                                    | 7.04, <i>d</i> (8.5) |  |
| Gly              | εCH/ηCH          | 116.5                | 6.71, <i>d</i> (8.5)                     | 116.2                | 6.69, <i>d</i> (8.5)                     |
|                  | ζC               | 157.8                |  | 157.1                |  |
|                  | NH               |                      | 8.18, <i>d</i> (10.0)                    |                      | 8.18                                     |
|                  | CO               | 172.0                |  | 172.0                |  |
| Thr              | αCH <sub>2</sub> | 44.3                 | 3.74, <i>d</i> (17.1)                    | 44.0                 | 3.72, <i>d</i> (17.0)                    |
|                  |                  |                      | 4.27, <i>d</i> (17.1)                    |                      | 4.25, <i>d</i> (17.0)                    |
|                  |                  |                      | 8.13, <i>d</i> (6.3)                     |                      | 8.16                                     |
|                  | NH               |                      | 8.13, <i>d</i> (6.3)                     |                      | 8.16                                     |
| Gly              | CO               | 172.0                |  | 172.0                |  |
|                  | αCH <sub>2</sub> | 44.3                 | 3.74, <i>d</i> (17.1)                    | 44.0                 | 3.72, <i>d</i> (17.0)                    |
|                  |                  |                      | 4.27, <i>d</i> (17.1)                    |                      | 4.25, <i>d</i> (17.0)                    |
|                  |                  |                      | 8.13, <i>d</i> (6.3)                     |                      | 8.16                                     |
| Thr              | CO               | 172.3                |  | 172.3                |  |
|                  | αCH              | 57.1                 | 4.89, <i>d</i> (3.1)                     | 57.1                 | 4.87, <i>d</i> (3.1)                     |
|                  | βCH              | 70.7                 | 4.52, <i>dq</i> (3.1, 6.1)               | 70.8                 | 4.50, <i>dq</i> (3.1, 6.3)               |
|                  | γCH <sub>3</sub> | 19.7                 | 1.23 <i>d</i> (6.1)                      | 19.7                 | 1.21 <i>d</i> (6.3)                      |
|                  |                  | 7.42 <i>d</i> (9.9)  |  | 7.44 <i>d</i> (9.9)  |  |

TyrNH and Met(O)(CO), GlyH<sub>2</sub>-α and Tyr(CO), ThrNH and Gly(CO)) allowed us to determine the planar structure of 1, as shown in Fig. 1. Squamin D (2) showed the same molecular formula as 1, C<sub>37</sub>H<sub>56</sub>N<sub>8</sub>O<sub>11</sub>S, according to ESI-HRMS results that displayed a peak at *m/z* 843.3668 [M+Na]<sup>+</sup>. Detailed analysis of its <sup>1</sup>H and <sup>13</sup>C NMR data, assisted by 2D NMR spectroscopy, established the planar structure of 2 as identical to 1. However, slight variations between the NMR chemical shifts of the two compounds were found, particularly involving the methylsulfinyl group (Table 1). Sulfoxide groups can be considered as asymmetric centers, due to their high activation energies for inversion (162–197 kJ mol<sup>-1</sup>) that prevent enantiomers interconverting (Marom et al., 2007). Therefore, we concluded that 1 and 2 were a pair of diastereoisomers with

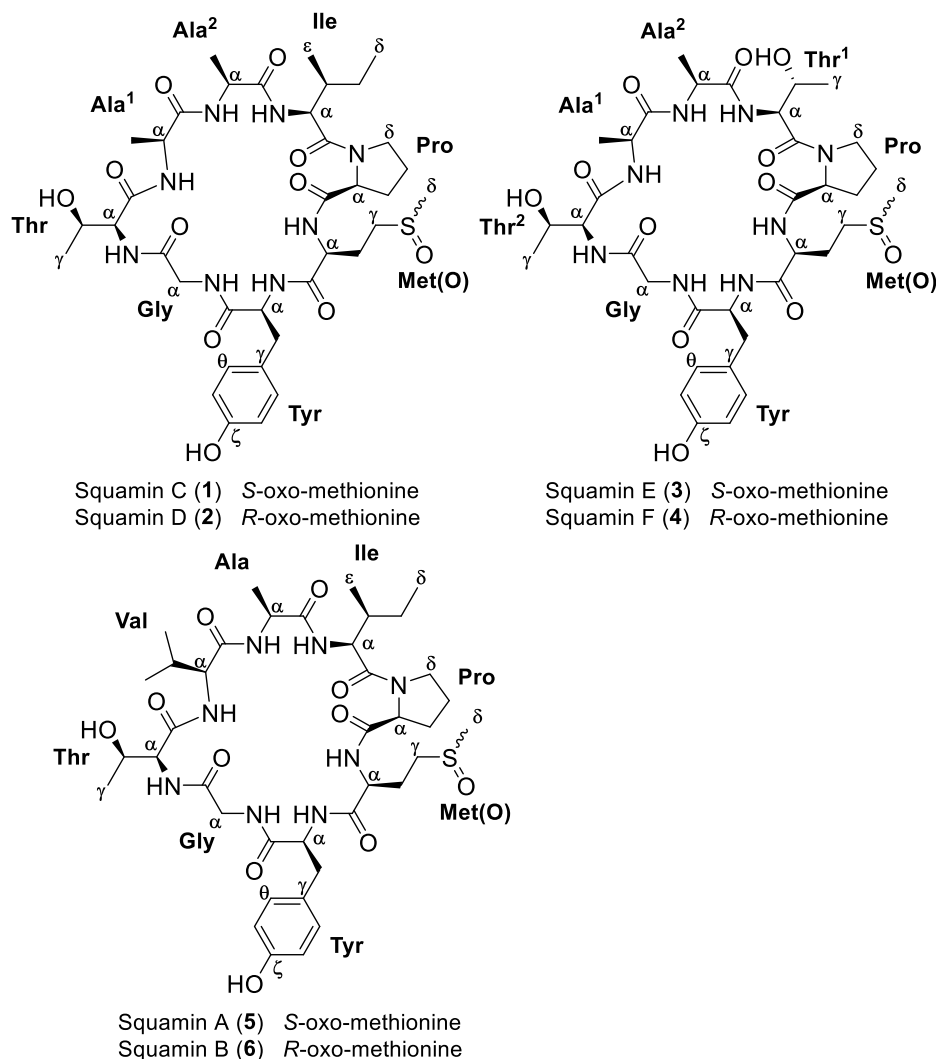


Fig. 1. Structure of squamins A-F (1–6).

different configurations at the sulfoxide stereogenic center.

Two closely related metabolites, squamins E (3) and F (4), were also isolated in this study. Analysis of their ESI-HRMS data showed peaks at  $m/z$  831.3330  $[M+Na]^+$  for 3 and  $m/z$  831.3325  $[M+Na]^+$  for 4, both corresponding to a molecular formula of  $C_{35}H_{52}N_8O_{12}S$ . A detailed structural analysis of these compounds suggested a partial amino acid sequence -Pro-Met(O)-Tyr-Gly-Thr<sup>2</sup>-Ala<sup>1</sup>-Ala<sup>2</sup>-, identical to those observed in squamins C (1) and D (2). However, the experimental data indicated the presence of a new threonine residue, replacing the previously described isoleucine residue in 1 and 2. The <sup>1</sup>H NMR spectra for the new Thr<sup>1</sup> were assigned commencing from H<sub>3</sub>-γ ( $\delta_H$  1.14, d,  $J = 6.5$  Hz), which was coupled with methine H-β ( $\delta_H$  4.25, dq,  $J = 2.4, 6.5$  Hz). This was sequentially connected with the proton of methine H-α ( $\delta_H$  4.64, d,  $J = 2.4$  Hz). The new threonine residue was linked using the HMBC experiment, where the proton Thr<sup>1</sup>H-α was correlated with Ala<sup>2</sup> (CO,  $\delta_C$  176.3). The signal corresponding to ProH-α (4.74, t,  $J = 8.2$  Hz) was also connected with Thr<sup>1</sup>(CO) ( $\delta_C$  173.4) (Table 2).

A literature search revealed that two similar molecules, squamins A and B (5–6), had been isolated from *Annona squamosa* L. (Annonaceae) (Zhi-Da et al., 2000; Ren-Wang et al., 2003). Squamins C and D (1–2) show an alanine residue in place of the valine residue present in 5 and 6. Squamins E and F (3–4), in addition to the previous substitution, incorporate a new threonine residue instead of the characteristic isoleucine in 5 and 6.

Absolute configurations of the amino acid residues were established

Table 2

NMR data (CD<sub>3</sub>OH) for amino acid sequence, -Ala<sup>2</sup>-Thr<sup>1</sup>-Pro-, of squamin E (3) and F (4).

| Amino acid       | Position         | Squamin E (3) |                                 | Squamin F (4) |                                 |
|------------------|------------------|---------------|---------------------------------|---------------|---------------------------------|
|                  |                  | $\delta_C$    | $\delta_H$ , mult. ( $J$ in Hz) | $\delta_C$    | $\delta_H$ , mult. ( $J$ in Hz) |
| Ala <sup>2</sup> | CO               | 176.3         |                                 | 176.2         |                                 |
|                  | αCH              | 52.4          | 4.25, q (7.4)                   | 52.4          | 4.23, q (7.4)                   |
|                  | βCH <sub>3</sub> | 17.6          | 1.49, d (7.4)                   | 17.6          | 1.47, d (7.4)                   |
|                  | NH               |               | 7.77, bs                        |               | 7.69, bs                        |
| Thr <sup>1</sup> | CO               | 173.4         |                                 | 173.6         |                                 |
|                  | αCH              | 54.9          | 4.64, d (2.4)                   | 54.9          | 4.68, d (2.9)                   |
|                  | βCH              | 68.7          | 4.25, dq (2.4, 6.5)             | 68.8          | 4.31, dd (2.9, 6.5)             |
| Pro              | γCH <sub>3</sub> | 20.2          | 1.14, d (6.5)                   | 20.2          | 1.17, d (6.5)                   |
|                  | NH               |               | 7.37, d (9.6)                   |               | 7.38, d (9.6)                   |
|                  | CO               | 177.5         |                                 | 177.2         |                                 |
|                  | αCH              | 64.2          | 4.74, t (8.2)                   | 64.3          | 4.73, t (8.2)                   |
|                  | βCH <sub>2</sub> | 1.91, m       |                                 | 30.7          | 1.91, m                         |
|                  |                  | 2.35, m       |                                 |               | 2.36, m                         |
| γCH <sub>2</sub> | 26.0             | 2.04, m       | 25.9                            | 2.05, m       |                                 |
|                  |                  | 2.08, m       |                                 | 2.08, m       |                                 |
| δCH <sub>2</sub> | 48.8             | 3.54, m       | 49.0                            | 3.55, m       |                                 |
|                  |                  | 3.68, m       |                                 | 3.67, m       |                                 |

by a modified version of Marfey's method (Bhushan and Brückner, 2004). Thus, each compound (1–4) was first hydrolyzed using HCl and subsequently each hydrolysate was derivatized using  $N\alpha$ -(2,4-dinitro-5-fluorophenyl)-L-alaninamide (*L*-FDLA). The chromatographic retention times of these FDLA amino-acid derivatives were established by HPLC, monitored by UV absorption at 340 nm. All FDLA derivatives were identified by comparison of their HPLC retention times with those measured for amino-acid standards. The absolute configurations of the amino-acid residues of 1–4 were all identified as *L*. However, regarding the configuration of the methionine oxide residues, it has to be noted that sulfoxides are quickly racemized in HCl solution (Mislow et al., 1994), such as that used for peptide hydrolysis in Marfey's analyses. Consequently, the rapid interconversion between the *L*-Met ( $R^*/S^*$ )-oxides in acid conditions made it impossible to assign a configuration to the sulfoxide groups in compounds 1–4. Although a number of methods to determine the configuration of chiral sulfoxides have been described, it is still far from a routine matter to establish them reliably. The comparison between experimental and calculated values have been successfully used to address complex stereochemical problems involving natural products (Li et al., 2020; Daranas and Sarotti, 2021; Domínguez et al., 2014), without the need of a total synthesis (Kutateladze and Holt, 2019). In fact, this approach has been successfully used on chiral sulfoxides (Li et al., 2008). Methods based on Bayes' theorem such as DP4, DP4+ or *J*-DP4 stand out (Smith and Goodman, 2010; Grimblat et al., 2015; Grimblat et al., 2019). Moreover, specific methodologies have been proposed to assign the configuration of groups of stereoisomers when experimental NMR data is available for all of them, as for squamins 1–6 (Smith and Goodman 2009). Specifically, the recently proposed statistical parameter MAE $_{\Delta\Delta\delta}$  (MAE = Mean Average Error) calculates differences between the experimental and calculated NMR data for groups of stereoisomers, reducing systematic errors and providing a more robust assignment than DP4-based methods in these cases (Lauro et al., 2020). Nevertheless, the great similarity observed in the NMR data experimentally measured for all pairs of squamin stereoisomers studied here makes this approach very challenging. In effect, the resemblance between the experimental NMR data of 1 and 2 suggests that both compounds adopt a similar conformation. They mainly diverge only in the configuration of the sulfoxide group, as observed in their crystalline structures. Thus, the crystallographic structures of squamins A (5) (CCDC 196170) and B (6) (CCDC 196169) were used to test if the previously mentioned approach could be useful for these molecules (Ren-Wang et al., 2003).

First, both structures were geometrically optimized using the B3LYP/6-31G(d) functional/basis set. Next,  $^1\text{H}$  and  $^{13}\text{C}$  NMR chemical shifts for the two structures were calculated at the MPW1PW91/6-31 + G(d,p) level of theory. Finally, the MAE $_{\Delta\Delta\delta}$  parameter was calculated for the two possible experimental/calculated comparisons. As a result, an *S* configuration turned out to be the most likely answer for compound 5, while an *R* configuration should be proposed for compound 6 (Table 3). Importantly, our result agrees with a previous proposal made for 5, where the configuration of the sulfoxide group was also determined as *S* based on a chemical shift comparison with a standard sample of *S*-oxo-

methionine (Shi et al., 1999). The structures of squamins C (1) and D (2) were built using the crystallographic coordinates of compounds 5 and 6, but modifying the valine to an alanine residue. Next, quantum mechanical NMR calculations and the previously described analysis were undertaken. As a result, an *S* configuration was found for compound 1 and an *R* for compound 2. Finally, the same procedure was applied to squamins E (3) and F (4). Despite the 3D structures for 3 and 4 adopting a preferential conformation similar to other squamins, the configuration at the sulfoxide could not be assured (Fig. 2). The reason was that the MAE $_{\Delta\Delta\delta}$  parameter calculated using  $^1\text{H}$  data pointed to an *S* configuration for compound 3 and an *R* for compound 4, but the opposite was found using the  $^{13}\text{C}$  NMR data (Table 3 and S17-S19). In order to solve this discrepancy, experimental data were compared. This showed that the  $^1\text{H}$  NMR chemical shift measured for the methyl group of the oxo-methionine residue was 2.35 ppm in squamin A (5), 2.34 ppm in squamin C (1) and 2.36 ppm in squamin E (3), indicating that all of them share the same *S* configuration. On the other hand, squamins B (6), D (2) and F (4) showed signals above 2.5 ppm, indicating that all three share the *R* configuration.

### 2.3. Biological activity

Cyclopeptides show a variety of biological properties; among these their cytotoxicity is important (Anaya-Esparza et al., 2020). Therefore, the *in vitro* cytotoxic activity of squamins C–F (1–4) was assessed using XTT assays and two cancer cell lines: DU-145 (human prostate cancer) and HeLa (human cervical carcinoma) (Cen-Pacheco et al., 2012). As shown in Table 4, all these compounds were able to inhibit cell proliferation at  $\mu\text{M}$  concentration.

### 3. Conclusions

In conclusion, the structures of four previously undescribed cyclopeptides, named squamins C–F (1–4), were determined by the combined use of computational and spectroscopic techniques (QM-NMR) as well as a modified version of Marfey's chromatographic method. Compounds 1–4 turned out to be two pairs of conformational isomers that differed in the configuration of an asymmetric sulfoxide group, characteristic of methionine oxide residues. Squamins C–F (1–4) are structurally related to the squamins A and B (5–6), epimers previously isolated from *A. squamosa*. All compounds were active against the cell lines DU-145 (prostate cancer) and HeLa (human cervical carcinoma) in the range 8–25  $\mu\text{M}$ . These results suggested that this type of compounds could be candidates in the search for lead therapeutic compounds. Clearly, *A. globiflora* is an important source of bioactive molecules, which could

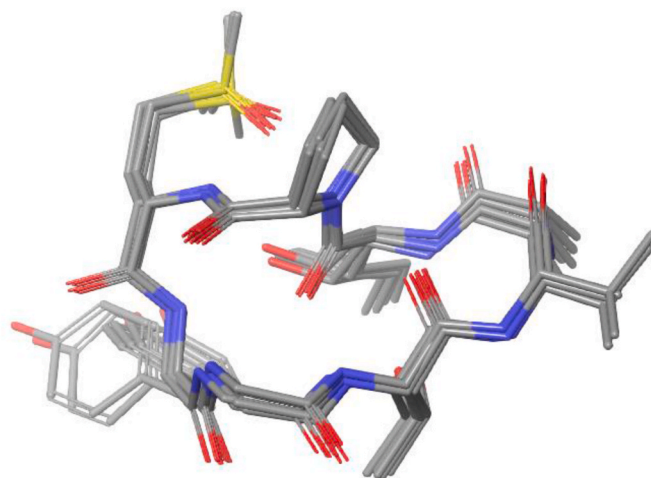


Fig. 2. Optimized geometries of squamins A-F (1–6) at B3LYP/6-31G(d) functional/basis set.

Table 3

MAE value for two sets of experimental/calculated data for squamins A-B, C-D and E-F.

| Squamins A&B                             | calcA-B/exp1-2 | calcA-B/exp2-1 |
|--|----------------|----------------|
| MAE $_{\Delta\Delta\delta}^{13}\text{C}$ | 1.09           | 1.23           |
| MAE $_{\Delta\Delta\delta}^1\text{H}$    | 0.23           | 0.24           |
| Squamins C&D                             | calcA-B/exp1-2 | calcA-B/exp2-1 |
| MAE $_{\Delta\Delta\delta}^{13}\text{C}$ | 1.13           | 1.17           |
| MAE $_{\Delta\Delta\delta}^1\text{H}$    | 0.20           | 0.22           |
| Squamins E&F                             | calcA-B/exp1-2 | calcA-B/exp2-1 |
| MAE $_{\Delta\Delta\delta}^{13}\text{C}$ | 0.92           | 0.76           |
| MAE $_{\Delta\Delta\delta}^1\text{H}$    | 0.10           | 0.12           |

**Table 4**

*In vitro* growth inhibitory activity of compounds 1–4 on human tumor cells. IC<sub>50</sub> are means of three experiments.

| Compound    | IC <sub>50</sub> (μM ± SD) |             |
|-------------|----------------------------|-------------|
|             | DU-145                     | HeLa        |
| 1           | 12.1 ± 2.91                | 20.8 ± 3.15 |
| 2           | 18.1 ± 3.01                | 10.9 ± 1.88 |
| 3           | 11.7 ± 3.70                | 19.1 ± 3.00 |
| 4           | 8.8 ± 3.77                 | 24.7 ± 1.89 |
| Doxorubicin | 1.3 ± 0.51                 | 0.8 ± 0.27  |

promote the sustainable exploitation of this undervalued species.

## 4. Experimental

### 4.1. General experimental procedures

Optical rotation was determined on a Perkin–Elmer 241 polarimeter (Waltham, MA, USA), using a sodium lamp operating at 589 nm. NMR spectroscopy was performed on Bruker AVANCE 600 MHz instruments using CD<sub>3</sub>OD and CD<sub>3</sub>OH at 298 K, and coupling constants are given in Hz. The NMR, COSY, HSQC-TOCSY, HSQC and HMBC data were acquired using standard pulse sequences. <sup>3</sup>J<sub>H,H</sub> values were measured from 1D <sup>1</sup>H NMR. NMR data were processed using MestReNova software (v 11.01, Santiago de Compostela, Spain). Mass spectra were recorded on a VG AutoSpec FISON spectrometer (Danvers, MA, USA). HPLC separations were carried out with an LKB 2248 system (LKB-Producter AB, Bromma, Sweden) equipped with a photodiode array detector. All of the solvents used were HPLC-grade. HPLC was monitored by TLC, performed on AL Si gel Merck 60 F254 (Kenilworth, NJ, USA). TLC plates were visualized by UV light (365 nm) and phosphomolybdic acid solution 10 wt % in ethanol.

### 4.2. Plant materials

The seeds of *Annona globiflora* Schlttdl. (Annonaceae) were collected from the municipality Medellín de Bravo, Veracruz Ignacio de la Llave (México) in May 2018 (wet season) (19°01'44.5"N 96°08'20.4"W) and identified by taxonomists of the Institute for Biological Research at Veracruz University. After collection, the biological material was dried at room temperature for one week, and then triturated using a steel blender (particle size 0.1–0.5 cm).

### 4.3. Extraction and chromatographic separation

*Annona globiflora* seeds (500 g) were extracted with MeOH (4 × (3L × 3 h) at room temperature and the solvent removed *in vacuo* to give a brownish viscous oil (AGS-1 12.5 g). The methanolic extract was first fractioned for liquid-liquid extraction using a modified Kupchan method (Kupchan et al., 1973; Cen-Pacheco et al., 2019a,b). The ethyl acetate fraction (AGS-1C; 416 mg) was chromatographed at medium pressure in a Lobar LiChroprep-RP18, eluted with MeOH/H<sub>2</sub>O (6:4) at 2.5 mL/min flow. Fractions collected between 19 and 24 min, and 25–28 min were pooled together (AGS-1C6 and AGS-1C7 19.7 and 21.5 mg, respectively). Both fractions (AGS-1C6 and 1C7) were finally purified in a μ-BondapakTM C-18 (1.9 Ø x 15 cm) HPLC column, using H<sub>2</sub>O/MeOH (7:3 or 8:2) as mobile phase at 1 mL/min, to afford pure squamin C (1) (2.9 mg), squamin D (2) (2.5 mg), squamin E (3) (1.9 mg) and squamin F (4) (1.5 mg).

#### 4.3.1. Squamin C (1)

Amorphous white solid; [α]<sub>D</sub><sup>25</sup> -52 (c = 0.29, MeOH); ESI-MS *m/z* 856.4, 843.4, 821.3, 579.3, 433.2, 413.3; ESI-HRMS *m/z* 843.3691 [M+Na]<sup>+</sup> (calc for C<sub>37</sub>H<sub>56</sub>N<sub>8</sub>O<sub>11</sub>NaS *m/z* 843.3687); <sup>1</sup>H (600 MHz, CD<sub>3</sub>OD) and <sup>13</sup>C NMR (125 MHz, CD<sub>3</sub>OD) data in CD<sub>3</sub>OD are given in

**Table 1.**

#### 4.3.2. Squamin D (2)

Amorphous white solid; [α]<sub>D</sub><sup>25</sup> -48 (c = 0.25, MeOH); ESI-MS *m/z* 845.4, 844.4, 843.4, 450.2, 413.3; ESI-HRMS *m/z* 843.3668 [M+Na]<sup>+</sup> (calc for C<sub>37</sub>H<sub>56</sub>N<sub>8</sub>O<sub>11</sub>NaS *m/z* 843.3687); <sup>1</sup>H (600 MHz, CD<sub>3</sub>OD) and <sup>13</sup>C NMR (125 MHz, CD<sub>3</sub>OD) data in CD<sub>3</sub>OD are given in Table 1.

#### 4.3.3. Squamin E (3)

Amorphous white solid; [α]<sub>D</sub><sup>25</sup> -42 (c = 0.19, MeOH); ESI-MS *m/z* 833.3, 832.3, 831.3, 676.3, 675.3, 427.2; ESI-HRMS *m/z* 831.3330 [M+Na]<sup>+</sup> (calc for C<sub>35</sub>H<sub>52</sub>N<sub>8</sub>O<sub>12</sub>NaS *m/z* 831.3323); <sup>1</sup>H (600 MHz, CD<sub>3</sub>OD) and <sup>13</sup>C NMR (125 MHz, CD<sub>3</sub>OD) data in CD<sub>3</sub>OD are given in Table S3.

#### 4.3.4. Squamin F (4)

Amorphous white solid; [α]<sub>D</sub><sup>25</sup> -41 (c = 0.15, MeOH); ESI-MS *m/z* 833.3, 832.4, 831.3, 675.3, 463.3, 427.2; ESI-HRMS *m/z* 831.3325 [M+Na]<sup>+</sup> (calc for C<sub>35</sub>H<sub>52</sub>N<sub>8</sub>O<sub>12</sub>NaS *m/z* 831.3323); <sup>1</sup>H (600 MHz, CD<sub>3</sub>OD) and <sup>13</sup>C NMR (125 MHz, CD<sub>3</sub>OD) data in CD<sub>3</sub>OD are given in Table S4.

### 4.4. Marfey's analysis

Samples of squamins C–F (1–4) (400 μg) were hydrolyzed in 200 μL 6 N HCl at 50 °C for 24 h. After the residual HCl was removed *in vacuo*, to the residues was added 100 μL of an acetone solution containing 0.1 M of NaHCO<sub>3</sub> and 25 μg of 1-fluoro-2,4-dinitrophenyl-5-d-alaninamide (L-FDAA). The solution was heated at 75 °C for 4 h. Next, the reaction mixtures were cooled, neutralized with 2 N HCl (50 μL) and dissolved in MeOH (200 μL). Ten μL of each solution of FDLA derivatives was analyzed by HPLC. Additionally, standards of Gly, L-Ala, L-Thr, L-Ile, L-Pro, L-Met(O), L-Tyr (Sigma-Aldrich) were treated with L-FDAA as described above. The L-FDAA derivative of the L-amino acid standard was analyzed by HPLC-UV, and the retention times L-FDAA (8.16 min), Gly (5.80 min), L-Ala (6.60 min), L-Thr (4.84 min), L-Ile (12.49 min), L-Pro (7.35 min), L-Met(O) (4.17 min), L-Tyr (15.97 min) were compared with the Marfey's derivative of 1–4. HPLC conditions: a 5 μm X-Bridge® C-18 column (100 × 4.6 mm) maintained at 40 °C was operated at 0.8 mL/min with a gradient elution profile of CH<sub>3</sub>CN/H<sub>2</sub>O (2:8; acidified with 0.05% HCOOH) to CH<sub>3</sub>CN/H<sub>2</sub>O (6:4; acidified with 0.05% HCOOH) over 45 min, monitoring at 340 nm.

### 4.5. Cell culture

DU-145 (prostate cancer) and HeLa (human cervical carcinoma) cells were maintained in DMEM culture medium containing 10% (v/v) heat-inactivated fetal bovine serum (FBS), 2 mM L-glutamine, 100 U/mL penicillin, and 100 μg/mL streptomycin at 37 °C in air containing 95% humidity and 5% CO<sub>2</sub>. Cells were periodically tested for *Mycoplasma* infection using the MycoAlert® Mycoplasma detection kit (Lonza, Basel, Switzerland) as well as the Venor®GeM Advance Mycoplasma PCR detection Kit (Minerva Biolabs, Berlin, Germany), and found to be negative.

### 4.6. Preparation of samples for assay

Squamins C–F (1–4) were dissolved initially in DMSO at 40 mM, i.e., 400 times the maximum test concentration. For each test compound, the cells were exposed to serial decimal dilutions in the range of 10<sup>-4</sup> to 10<sup>-9</sup> M for a period of 48 h. Doxorubicin used as a positive control rendered IC<sub>50</sub> values in the order of 10<sup>-6</sup> – 10<sup>-7</sup> M and 0.25% DMSO as negative control.

#### 4.7. Cell growth inhibition assay

The effect of each compound on the proliferation of human tumor cell lines was determined using the XTT (sodium 3'-[1-(phenylaminocarbonyl)-3,4-tetrazolium]-bis (4-methoxy-6-nitro) benzene sulfonic acid hydrate) cell proliferation kit (Roche Molecular Biochemicals, Mannheim, Germany), as previously described (Cen-Pacheco et al., 2012). Cells ( $1.5\text{--}5.0 \times 10^3$  in 100  $\mu\text{L}$ ) were incubated in DMEM culture medium containing 10% heat-inactivated FBS, in the absence and presence of the indicated compounds at a concentration range of  $10^{-4}$  to  $10^{-9}$  M, in 96-well flat-bottomed microtiter plates. Following 72 h of incubation at 37 °C in a humidified atmosphere of air/CO<sub>2</sub> (19/1), the XTT assay was performed. Measurements were made in triplicate, and each experiment was also repeated three times. The IC<sub>50</sub> (50% inhibitory concentration) value, defined as the drug concentration required to cause 50% inhibition of cell proliferation with respect to the untreated controls, was determined for each compound. Data are shown as means  $\pm$  standard deviation (SD) of three independent experiments, each performed in triplicate.

#### 4.8. Computational details

QM-NMR calculations followed the approach previously described by Lauro et al. This relies on establishing the statistical MAE <sub>$\Delta\delta$</sub>  parameter, defined as

$$MAE_{\Delta\delta} = \frac{\sum (\Delta\delta)}{n_{\Delta\delta}}$$

obtained from the summation ( $\Sigma$ ) of the  $n$  computed absolute  $\delta$  error values ( $\Delta\delta$ ), normalized to the number of  $\Delta\delta$  errors considered ( $n$ ).

The crystallographic structures for squamins A (CCDC 196170) and B (CCDC 196169) were optimized at the B3LYP/6-31G (d) level of theory. These optimized structures were then used to obtain the calculated magnetic shielding constants ( $\sigma$ ) at the mPW1PW91/6-31 + G(d,p) level of theory. Subsequently, unscaled chemical shifts ( $\delta_u$ ) were calculated using TMS as reference standard according to the expression  $\delta_u = \sigma_0 - \sigma_x$ , where  $\sigma_x$  is the shielding tensor and  $\sigma_0$  is the shielding tensor of TMS computed at the same level of theory used to calculate  $\sigma_x$ . The structures of squamins C–F (1–4) were built using the crystallographic coordinates of compounds 5 and 6 as templates, making the necessary modifications in selected amino acids. Afterward, the resulting structures were geometrically optimized at the B3LYP/6-31G (d) level of theory. Due to the large size of the molecules, availability of crystallographic structures for 1–2 and the resemblance of their NMR data with those of 3–6 (which suggests that all of them adopt very similar conformations) computational studies were undertaken using only single conformations for each compound.

As all comparisons are between two sets of calculated data (A, B) and two sets of experimental data (1, 2), the number of possible comparisons for each pair of data is two (AB/12 and AB/21). For each comparison,  $\Delta\delta_{\text{calc}}$  and  $\Delta\delta_{\text{exp}}$  parameters are calculated using the equation  $\Delta\delta_{\text{calcA-B}} = \delta_{\text{calcA}} - \delta_{\text{calcB}}$ , where  $\delta_{\text{calcA}}$  and  $\delta_{\text{calcB}}$  are chemical shifts calculated for A and B data sets. This procedure is also followed to calculate  $\Delta\delta_{\text{exp}}$ . Finally, the specific  $\Delta\delta_{\text{calc}}$  and  $\Delta\delta_{\text{exp}}$  values are compared atom by atom, using the  $\Delta\Delta\delta$  parameter defined as  $\Delta\Delta\delta = |\Delta\delta_{\text{calc}} - \Delta\delta_{\text{exp}}|$ . The  $\Delta\Delta\delta$  parameter detects similarities between calculated and experimental data sets and is used for calculating the MAE <sub>$\Delta\delta$</sub>  parameter (Table 3 and S17–S19).

#### Declaration of competing interest

The authors declare that they have no known competing financial interests or personal relationships that could have appeared to influence the work reported in this paper.

#### Acknowledgments

This work was supported by the Government of the State of Veracruz de Ignacio de la Llave, Veracruz Council for Scientific Research and Technological Development [COVEICYDET, grant number 14 1953/2021], and by the Spanish Ministry of Science and Innovation (PID2019-109476RB-C21). This study made use of the CESGA and SGAI-CSIC supercomputing facilities. We thank G. Jones for English text edition, funded by Cabildo de Tenerife, TFinnova Program supported by MEDI and FDCAN.

#### Appendix A. Supplementary data

Supplementary data to this article can be found online at <https://doi.org/10.1016/j.phytochem.2021.112839>.

#### References

- Anaya-Esparza, L.M., García-Magaña, M.L., Domínguez-Ávila, J.A., Yahia, E.M., Salazar-López, N.J., González-Aguilar, G.A., Montalvo-González, E., 2020. Annonas: underutilized species as a potential source of bioactive compounds. *Food Res. Int.* 138, 109775. <https://doi.org/10.1016/j.foodres.2020.109775>.
- Bhushan, R., Brückner, H., 2004. Marfey's reagent for chiral amino acid analysis: a review. *Amino Acids* 27 (3–4), 231–247. <https://doi.org/10.1007/s00726-004-0118-0>.
- Capon, R.J., 2020. Extracting value: mechanistic insights into the formation of natural product artifacts - case studies in marine natural products. *Nat. Prod. Rep.* 37, 55–79. <https://doi.org/10.1039/C9NP00013E>.
- Cen-Pacheco, F., Mollinedo, F., Villa-Pulgarín, J.A., Norte, M., Fernández, J.J., Hernández Daranas, A., 2012. Saiyacenols A and B: the key to solve the controversy about the configuration of aplysiols. *Tetrahedron* 68 (39), 7275–7279. <https://doi.org/10.1016/j.tet.2012.07.005>.
- Cen-Pacheco, F., Ortiz-Celiseo, A., Peniche-Cardeña, A., Bravo-Ruiz, O., López-Fentanes, F.C., Valerio-Alfaro, G., Fernández, J.J., 2019a. Studies on the bioactive flavonoids isolated from *Azadirachta indica*. *Nat. Prod. Res.* 34 (24), 3483–3491. <https://doi.org/10.1080/14786419.2019.1579808>.
- Cen-Pacheco, F., Valerio-Alfaro, G., Santos-Luna, D., Fernández, J.J., 2019b. Sclerin, a new cytotoxic cyclononapeptide from *Annona scleroderma*. *Molecules* 24, 554. <https://doi.org/10.3390/molecules24030554>.
- Dahiya, R., Dahiya, S., 2021. Natural bioeffective cyclooligopeptides from plant seeds of *Annona* genus. *Eur. J. Med. Chem.* 214, 113221. <https://doi.org/10.1016/j.ejmech.2021.113221>.
- Daranas, A.H., Sarotti, A.M., 2021. Are computational methods useful for structure elucidation of large and flexible molecules? Belizentrin as a case study. *Org. Lett.* 23 (2), 503–507. <https://doi.org/10.1021/acs.orglett.0c04016>.
- Domínguez, H.J., Napolitano, J.G., Fernández-Sánchez, M.T., Cabrera-García, D., Novelli, A., Norte, M., Fernández, J.J., Daranas, A.H., 2014. Belizentrin, a highly bioactive macrocycle from the dinoflagellate *Prochloron* belizeanum. *Org. Lett.* 16 (17), 4546–4549. <https://doi.org/10.1021/ol502102f>.
- Escobedo-López, D., Campos-Rojas, E., Rodríguez-Núñez, J.R., Alía-Tejagal, I., Núñez-Colin, C.A., 2018. Priority areas to collect germplasm of *Annona* (annonaceae) in Mexico based on diversity and species richness indices. *Genet. Resour. Crop. Evol. Published online*. <https://doi.org/10.1007/s10722-018-0718-2>.
- Grimblat, N., Gavín, J.A., Daranas, A.H., Sarotti, A.M., 2019. Combining the power of J coupling and DP4 analysis on stereochemical assignments: The J-DP4 methods. *Org. Lett.* 21 (11), 4003–4007. <https://doi.org/10.1021/acs.orglett.9b01193>.
- Grimblat, N., Zanardi, M.M., Sarotti, A.M., 2015. Beyond DP4: an improved probability for the stereochemical assignment of isomeric compounds using quantum chemical calculations of NMR shifts. *J. Org. Chem.* 80 (24), 12526–12534. <https://doi.org/10.1021/acs.joc.5b02396>.
- Hernández Vidal, L., López Moctezuma, H., Vidal Martínez, N.A., Ruiz Bello, R., Castillo Rocha, D.G., Chiquito Contreras, R.G., 2014. La situación de las Annonaceae en México: principales plagas, enfermedades y su Control. *Rev. Bras. Frutic.* 36, 44–54. <https://doi.org/10.1590/S0100-29452014000500005>.
- Kutateladze, A.G., Holt, T., 2019. Structure validation of complex natural products: time to change the paradigm. What did synthesis of alstofolinine A prove? *J. Org. Chem.* 84 (12), 8297–8299. <https://doi.org/10.1021/acs.joc.9b00969>.
- Kupchan, S.M., Tsou, G., Sigel, C.W., 1973. Datisacacin, a novel cytotoxic cucurbitacin 20-acetate from *Datisca glomerata*. *J. Org. Chem.* 38 (7), 1420–1421. <https://doi.org/10.1021/jo00947a041>.
- Lauro, G., Das, P., Riccio, R., Reddy, D.S., Bifulco, G., 2020. DFT/NMR approach for the configuration assignment of groups of stereoisomers by the combination and comparison of experimental and predicted sets of data. *J. Org. Chem.* 85 (5), 3297–3306. <https://doi.org/10.1021/acs.joc.9b03129>.
- Leite, D.O.D., Nonato, C.de F.A., Camilo, C.J., de Carvalho, N.K.G., da Nobrega, M.G.L.A., Pereira, R.C., da Costa, J.G.M., 2020. *Annona* genus: traditional uses, phytochemistry and biological activities. *Curr. Pharmaceut. Des.* 26 (33), 4056–4091. <https://doi.org/10.2174/1381612826666200325094422>.
- Li, S.W., Cuadrado, C., Yao, L.G., Daranas, A.H., Guo, Y.W., 2020. Quantum mechanical-NMR-aided configuration and conformation of two unreported macrocycles isolated

- from the soft coral lobophytum sp.: energy calculations versus coupling constants. *Org. Lett.* 22 (11), 4093–4096. <https://doi.org/10.1021/acs.orglett.0c01155>.
- Li, W., Hwang, D.J., Cremer, D., Joo, H., Kraka, E., Kim, J., Ross II, C.R., Nguyen, V.Q., Dalton, J.T., Miller, D.D., 2008. Structure determination of chiral sulfoxide in diastereomeric bicalutamide derivatives. *Chirality* 21 (6), 578–583. <https://doi.org/10.1002/chir.20642>.
- Marom, H., Biedermann, P.U., Agranat, I., 2007. Pyramidal inversion mechanism of simple chiral and achiral sulfoxides: a theoretical study. *Chirality* 19 (7), 559–569. <https://doi.org/10.1002/chir.20417>.
- Mislow, K., Simmons, T., Melillo, J.T., Ternay, A.L., 1994. The hydrogen chloride-catalyzed racemization of sulfoxides. *J. Am. Chem. Soc.* 86 (7), 1452–1453. <https://doi.org/10.1021/ja010661a048>.
- Ren-Wang, J., Yang, L., Zhi-Da, M., Qi-Tai, Z., 2003. Molecular structure and pseudopolymorphism of squamatin A from *Annona squamosa*. *J. molec. Struct.* 655 (1), 157–162. [https://doi.org/10.1016/S0022-2860\(03\)00227-8](https://doi.org/10.1016/S0022-2860(03)00227-8).
- Shi, J.X., Wu, H.M., He, F.H., Inoue, K., Min, Z.D., 1999. Squamin-A, novel cyclopeptide from *Annona squamosa*. *Chin. Chem. Lett.* 10, 299–302. [http://caod.oriprobe.com/articles/46023390/Squamin\\_A\\_Novel\\_Cyclopeptide\\_from\\_Annona\\_squamosa.htm](http://caod.oriprobe.com/articles/46023390/Squamin_A_Novel_Cyclopeptide_from_Annona_squamosa.htm).
- Smith, S.G., Goodman, J.M., 2009. Assigning the stereochemistry of pairs of diastereoisomers using GIAO NMR shift calculation. *J. Org. Chem.* 74 (12), 4597–4607. <https://doi.org/10.1021/jo900408d>.
- Smith, S.G., Goodman, J.M., 2010. Assigning stereochemistry to single diastereoisomers by GIAO NMR calculation: the DP4 probability. *J. Am. Chem. Soc.* 132 (37), 12946–12959. <https://doi.org/10.1021/ja105035r>.
- Unno, K., Kawewan, I., Nakagawa, H., Kodani, S., 2020. Heterologous expression of a cryptic gene cluster from *Grimontia marina* affords a novel tricyclic peptide grimoviridin. *Appl. Microbiol. Biotechnol.* 104 (12), 5293–5302. <https://doi.org/10.1007/s00253-020-10605-z>.
- Zhi-Da, M., Jian-Xia, S., Na, L., Qi-Tai, Z., Hou-Ming, W., 2000. Two conformational isomers of cyclopeptide from *Annona squamosa*. *J. China Pharm. Univ.* 31, 332–338. <http://www.zgykdx.cn/jcpu/article/abstract/200005159>.